Euro. Jnl of Applied Mathematics (2007), *vol.* 18, *pp.* 659–677.
doi:10.1017/S0956792507007206 Printed in the United Kingdom

Mathematical model of falling of a viscous jet onto a moving surface

A. HLOD, A. C. T. AARTS, A. A. F. VAN DE VEN and M. A. PELETIER

Center for Analysis, Scientific computing and Applications, Eindhoven University of Technology, Eindhoven, The Netherlands

(*Received 24 January 2007; revised 24 October 2007*)

The stationary flow of a jet of a Newtonian fluid that is drawn by gravity onto a moving surface is analyzed. It is assumed that the jet has a convex shape and hits the moving surface tangentially. The flow is modelled by a third-order ODE on a domain of unknown length and with an additional integral condition. By solving part of the equation explicitly, the problem is reformulated as a first-order ODE with an integral constraint. The corresponding existence region in the three-dimensional parameter space is characterized in terms of an easily calculable quantity. In a qualitative sense, the results from the model are found to correspond with experimental observations.

1 Introduction

In the flow of a viscous fluid jet falling onto a moving surface, different flow regimes can be distinguished, as is easily observed if one pours syrup onto a pancake (see Figs 1 and 2). If the syrup is poured from a large height and the bottle is moved slowly, the main part of the syrup thread between the bottleneck and the pancake remains steady and purely vertical, apart from boundary layers at the two ends (Fig. 1). We call *straight* for this flow type of the syrup. Another situation is possible if the bottle is held closer to the pancake and moved relatively faster. Then the syrup thread between the bottleneck and the pancake has a convex shape, apart from a possible bending boundary layer near the bottle, and touches the pancake tangentially (Fig. 2). We call *curved* for this type of syrup flow. Although the 'straight' case may seem just a special case of the 'curved' flow, simple experiments (and the analysis of our forthcoming paper [6]) show that both types of flow occur in open sets in parameter space.

There is a large body of literature on viscous jets or sheets that impinge upon *fixed* surfaces, where one can observe unstable behaviour [14]; i.e. folding of viscous sheets [13, 9, 17], coiling of viscous jets [10], and viscous fluid buckling [4, 15]. The first published study of a viscous jet falling onto a *moving* surface was done by Chiu-Webster and Lister [2]. They performed an extensive set of experiments studying steady and unsteady viscous jet behaviour. The case of steady flow was modelled both in [2] and in the later publication [11].

The analysis of the previous publications, however, makes no distinction between the two types of steady flow mentioned above, curved and straight. In this paper, we study

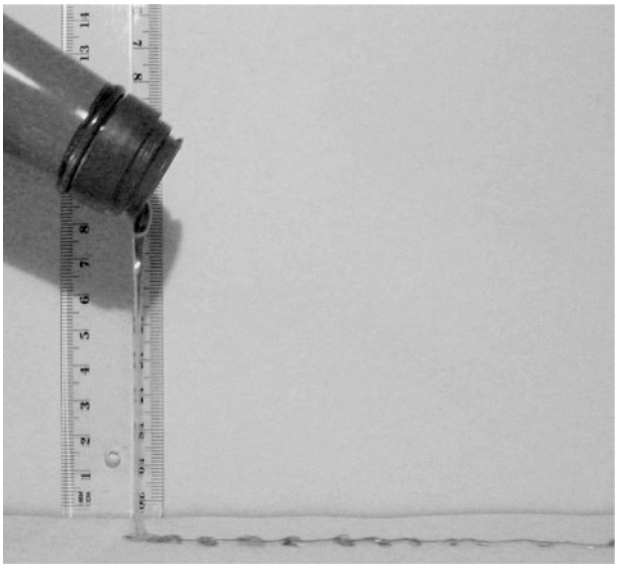

FIGURE 1. Straight flow of syrup for low surface velocity and large bottle height.

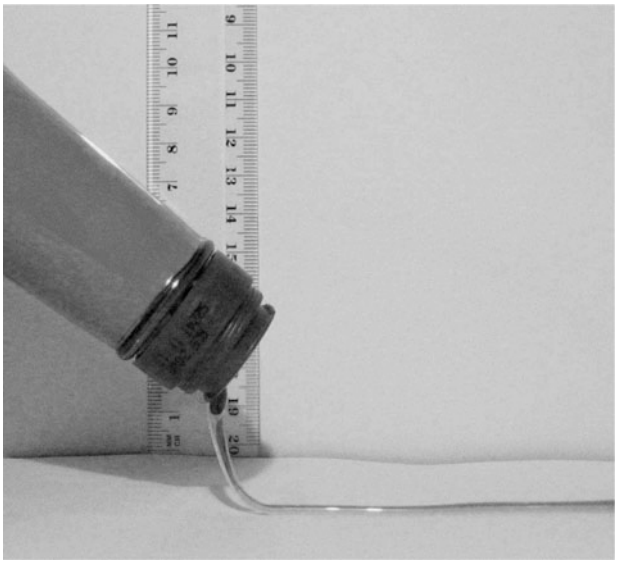

FIGURE 2. Curved flow of syrup for high surface velocity and small bottle height.

the curved case in full detail, as described by the model of [2], but we neglect surface tension and focus on the mathematical analysis. The main issue that we address here is the existence or non-existence of a steady, curved solution. This determines the parameter region in terms of falling height, surface velocity, flow velocity at the nozzle, fluid density, and viscosity, for which the jet is curved. By reformulating the problem as an algebraic

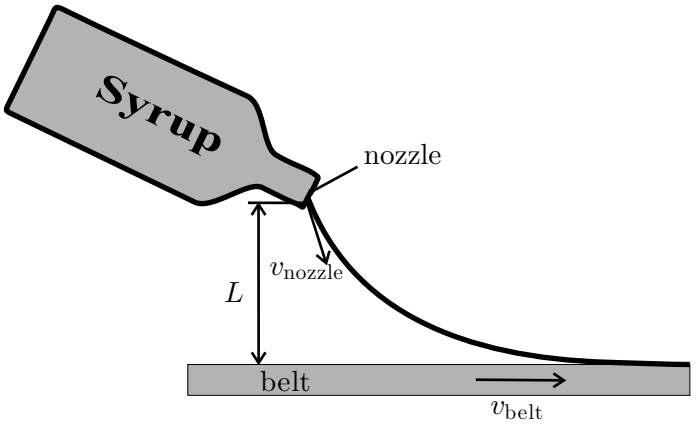

FIGURE 3. Jet falling from the nozzle onto the moving belt.

equation, we derive a particularly simple criterion (see Theorem 7) that characterizes the curved jet existence, or lack thereof, in terms of a single function of two variables. In addition, the formulation identifies a monotonic dependence on the model parameters. We show that the results obtained from our model qualitatively agree with the results of [2, 11].

In Section 2, we describe the model of the flow, where we first concentrate on the curved jet of Fig. 2. In Section 3, the original system of equations is transformed to a first-order differential equation for the flow velocity and two additional relations for two unknown parameters. In Section 4, we show that in a certain parameter regime the original system admits a unique solution, and we give a convenient characterization of the relevant part of parameter space. In Section 5, we present the solution algorithms for the model equations. Results for various model parameters are shown in Section 6. In Section 7, we present what happens with the jet if the curved jet does not exist, and how our model should be adjusted to describe the actual flow, and also provide a comparison with the existing results. In Section 8, we discuss our results and give some conclusions.

2 Mathematical model

A thin stream of Newtonian fluid with viscosity η and density ρ is falling from the nozzle of a bottle onto a moving belt (Fig. 3). We use the theory of thin jets (see e.g. [16]) and thus describe the jet as a curve. The magnitude of the flow velocity at the nozzle is v_{nozzle}, the belt velocity is v_{belt}, and the vertical distance between the nozzle and the belt is L. The flow of the fluid is stationary and the jet has a curved shape. We restrict ourselves to curves under tension and therefore require that

$$v_{\text{belt}} > v_{\text{nozzle}}. \tag{2.1}$$

In Lemma 1, we show that for a curved jet the flow velocity increases from the nozzle to the belt, which justifies (2.1).

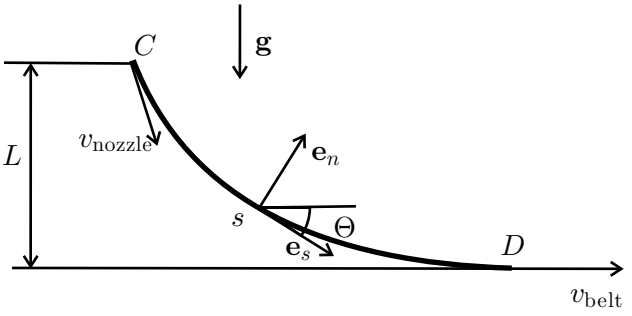

FIGURE 4. The geometry of the jet falling from the nozzle onto the moving belt.

The part of the jet between the nozzle and the belt is represented by its centre line, the curve CD in Fig. 4. Point C indicates that the nozzle and point D indicates the contact with the belt. The acceleration of gravity is $\mathbf{g}$ and the belt surface is perpendicular to $\mathbf{g}$. We parameterize the centre line by arclength s ($s = 0$ at C, and $s = s_{\text{end}}$ at D). For each point on the curve, we define a local orthonormal coordinate system $\mathbf{e}_s(s), \mathbf{e}_n(s)$ consisting of the tangent and normal unit vectors at the point s. The angle between $\mathbf{e}_s(s)$ and the belt surface is $\Theta(s)$. The cross-sectional area at s is $\mathscr{A}(s)$, and the average velocity of the fluid at this point is $\mathbf{v}(s) = v(s)\mathbf{e}_s(s)$.

The equations describing steady-state flow of fluid are obtained from [16, (4.18), p. 48] by neglecting the dynamic terms, the shearing force and the balance of momentum of momentum equation. The resulting system consist of the equations of conservation of mass and balance of momentum,

$$(\mathscr{A}(s)v(s))' = 0, \tag{2.2}$$

$$(\mathscr{A}(s)v(s)\mathbf{v}(s))' = \frac{1}{\rho}(P(s)\mathbf{e}_s(s))' + \mathbf{g}\mathscr{A}(s), \tag{2.3}$$

where by prime denotes differentiation with respect to s. The longitudinal force $P(s)$ is obtained from the constitutive law for a Newtonian viscous fluid,

$$P(s) = \eta_T \mathscr{A}(s)v'(s). \tag{2.4}$$

Here η_T is the Trouton elongational viscosity, which for a Newtonian fluid equals 3η [16].

Using (2.2) and (2.4), we write the balance of momentum (2.3) in components in the coordinate system $\mathbf{e}_s(s), \mathbf{e}_n(s)$, as

$$v'(s) = \frac{g\sin\Theta(s)}{v(s)} + 3\nu\left(\frac{v'(s)}{v(s)}\right)', \tag{2.5}$$

$$v(s)\Theta'(s) = \frac{g\cos\Theta(s)}{v(s)} + 3\nu\left(\frac{v'(s)}{v(s)}\right)\Theta'(s), \tag{2.6}$$

where ν is the kinematic viscosity, i.e. $\nu = \eta/\rho$.

Since system (2.5)–(2.6) is of second order with respect to the velocity $v(s)$ and of first order with respect to the angle $\Theta(s)$, we need two boundary conditions for $v(s)$ and one

for $\Theta(s)$. For $v(s)$, we know the velocity of the jet at the nozzle (point C) and the velocity at the contact with the belt (point D)

$$v(0) = v_{\text{nozzle}}, \tag{2.7}$$

$$v(s_{\text{end}}) = v_{\text{belt}}. \tag{2.8}$$

Note that the length s_{end} of the jet CD is unknown. The angle $\Theta(s)$ at the contact with the belt is zero, so

$$\Theta(s_{\text{end}}) = 0. \tag{2.9}$$

Because the length of the belt s_{end} is unknown in advance, we need an additional condition relating s_{end} to the distance L between the nozzle and the belt,

$$L = \int_0^{s_{\text{end}}} \sin\Theta(s)\, ds. \tag{2.10}$$

Equations (2.5) and (2.6) together with the three boundary conditions (2.7–2.9), and the additional condition (2.10) form the complete system for the unknowns $v(s)$, $\Theta(s)$, and s_{end}.

Next, we make the equations dimensionless. We scale the length s_{end} with respect to $3v/v_{\text{belt}}$, reverse the direction of s, and move the origin of s to point D, i.e. $\tilde{s} := v_{\text{belt}}(s_{\text{end}} - s)/(3v)$. The velocity $v(s)$ is scaled with respect to the velocity of the belt v_{belt}, i.e., $v_{\text{belt}}\tilde{v}(\tilde{s}) := v(s)$. Also we introduce a new angle $\tilde{\Theta}(\tilde{s}) := \Theta(s)$. The scaled version of (2.5)–(2.10) reads

$$\left(\tilde{v}(\tilde{s}) + \frac{\tilde{v}'(\tilde{s})}{\tilde{v}(\tilde{s})}\right)' = -A\frac{\sin\tilde{\Theta}(\tilde{s})}{\tilde{v}(\tilde{s})}, \tag{2.11}$$

$$\tilde{\Theta}'(\tilde{s}) = -A\frac{\cos\tilde{\Theta}(\tilde{s})}{\tilde{v}(\tilde{s})\left(\tilde{v}(\tilde{s}) + \frac{\tilde{v}(\tilde{s})'}{\tilde{v}(\tilde{s})}\right)}, \tag{2.12}$$

$$\tilde{v}(0) = 1, \tag{2.13}$$

$$\tilde{v}(\tilde{s}_{\text{end}}) = \tilde{v}_{\text{nozzle}}, \tag{2.14}$$

$$\tilde{\Theta}(0) = 0, \tag{2.15}$$

$$\int_0^{\tilde{s}_{\text{end}}} \sin\tilde{\Theta}(\tilde{s})\, d\tilde{s} = \text{Re}. \tag{2.16}$$

Here

$$A = \frac{3gv}{v_{\text{belt}}^3}, \qquad \text{Re} = \frac{v_{\text{belt}}L}{3v}, \qquad \tilde{v}_{\text{nozzle}} = \frac{v_{\text{nozzle}}}{v_{\text{belt}}}, \qquad \text{and} \qquad \tilde{s}_{\text{end}} = \frac{s_{\text{end}}v_{\text{belt}}}{3v}.$$

All these parameters are positive and Re is the Reynolds number. The parameter A can be written in terms of the Reynolds number and Froude number Fr as

$$A = \frac{1}{\text{Fr}^2\text{Re}}, \text{ where } \text{Fr} = \frac{v_{\text{belt}}}{\sqrt{Lg}}.$$

The prime now denotes differentiation with respect to $\tilde{s}$, and in the sequel we omit the tildes.

3 A first-order differential equation for the velocity

By introducing a new variable $\xi(s)$

$$\xi(s) = v(s) + \frac{v'(s)}{v(s)}, \tag{3.1}$$

we can rewrite the equations (2.11–2.12) as

$$v(s)\xi'(s) = -A\sin\Theta(s), \tag{3.2}$$

$$v(s)\Theta'(s) = -A\frac{\cos\Theta(s)}{\xi(s)}, \tag{3.3}$$

$$v'(s) = \xi(s)v(s) - v^2(s). \tag{3.4}$$

Note that (3.2)–(3.4) is a third-order ordinary differential equation and we shall therefore consider it as a dynamical system in its own right with s as the time-like variable.

For the variable $\xi(s)$, it is necessary to provide an initial value. To compute it, we need to know values of $v(s)$ and $v'(s)$ at the same point. Because we do not know a value of $v'(s)$ at any point we prescribe a value of $\xi(s)$ at $s = 0$,

$$\xi(0) = -\sqrt{w},\ w \geqslant 0. \tag{3.5}$$

Here we restrict ourselves to a negative initial value for ξ. Further in this section, see (3.17) and (3.18), we explain our choice of the form for the initial value for $\xi(s)$. The value w is unknown in advance and is determined by the requirement that a solution of (3.2)–(3.4) has to satisfy the conditions (2.16) and (2.14).

Next, we replace the material coordinate s by the time t, according to

$$ds = v(t)dt,$$

in the system of equations (3.2)–(3.4) together with the conditions (2.13)–(2.16) and (3.5), and we obtain

$$\xi'(t) = -A\sin\Theta(t), \tag{3.6}$$

$$\Theta'(t) = -A\frac{\cos\Theta(t)}{\xi(t)}, \tag{3.7}$$

$$v'(t) = \xi(t)v^2(t) - v^3(t), \tag{3.8}$$

$$\xi(0) = -\sqrt{w}, \tag{3.9}$$

$$\Theta(0) = 0, \tag{3.10}$$

$$v(0) = 1, \tag{3.11}$$

$$v(t_{\text{end}}) = v_{\text{nozzle}}, \tag{3.12}$$

$$\int_0^{t_{\text{end}}} v(t)\sin\Theta(t)\,dt = \text{Re}. \tag{3.13}$$

Here

$$t_{\text{end}} = \int_0^{s_{\text{end}}} \frac{ds}{v(s)}$$

represents the dimensionless time necessary to flow from the nozzle to the belt, which is unknown in advance.

To solve equations (3.6) and (3.7), we multiply (3.6) by $\sin\Theta(t)$ and (3.7) by $\xi(t)\cos\Theta(t)$ and add them, to obtain,

$$(\xi(t)\sin\Theta(t))' = -A. \tag{3.14}$$

We integrate (3.14) with respect to t and use the initial condition (3.10) to obtain

$$\xi(t)\sin\Theta(t) = -At. \tag{3.15}$$

By eliminating $\sin\Theta(t)$ from (3.15) and substituting it into (3.6), we derive the differential equation for $\xi(t)$

$$\xi'(t) = \frac{A^2 t}{\xi(t)}, \tag{3.16}$$

which has the solution

$$\xi(t) = \pm\sqrt{A^2t^2 + \xi(0)^2}. \tag{3.17}$$

Here we have to choose a correct branch of the square root (3.17). The branch with the positive sign gives negative $\sin\Theta(t)$, see (3.15), which implies an upward-sloping jet; the physically reasonable choice is, therefore, the branch with the negative sign. With the initial condition (3.5) we get

$$\xi(t) = -\sqrt{A^2t^2 + w}, \tag{3.18}$$

and from (3.15) and (3.18) we find

$$\Theta(t) = \arcsin\frac{At}{\sqrt{A^2t^2 + w}}. \tag{3.19}$$

Summarizing, the problem (3.6)–(3.13) simplifies to

$$v'(t) = -v^2(t)(\sqrt{A^2t^2 + w} + v(t)), \tag{3.20}$$

$$v(0) = 1, \tag{3.21}$$

$$v(t_{\text{end}}) = v_{\text{nozzle}}, \tag{3.22}$$

$$\int_0^{t_{\text{end}}} \frac{Atv(t)}{\sqrt{A^2t^2 + w}}\,dt = \text{Re}. \tag{3.23}$$

The unknowns of the problem (3.20)–(3.23) are the velocity $v(t)$ and the two positive parameters w and t_{end}.

4 Existence and uniqueness

We reformulate the problem (3.20)–(3.23) as an algebraic equation for the parameter w. First, we formulate properties of a solution $v(\cdot, w)$ of (3.20)–(3.21) for given $w \geqslant 0$.

Lemma 1 *For any $w \geqslant 0$, equation* (3.20) *has a unique solution $v(\cdot, w) : [0, \infty) \to (0, 1]$ satisfying* (3.21) *with $v(\cdot, w) \in C^1([0, \infty))$.*

In addition,

(1) *$v(t; w)$ is a strictly decreasing function of t for fixed w and a strictly decreasing function of w for fixed t.*

(2)

$$v(t;w) < \frac{2}{2 + t\sqrt{A^2t^2 + w}}. \tag{4.1}$$

(3) *The operator* $w \mapsto v(\cdot, w)$ *is continuous from* $[0,\infty)$ *to* $L^\infty(0,\infty)$.

Proof The right-hand side of (3.20) is $C(\Omega)$ and Lipshitz continuous in v uniformly on Ω, where $\Omega = (\{t, v, w\} : t \in [0,\infty), v \in (0,1], w \geqslant 0)$. Therefore, locally there exists a unique solution of (3.20) satisfying (3.21), which continuously depends on w [3, Theorem 7.4].

From (3.20) it follows that $v'(t;w) < 0$ whenever $v(t;w) > 0$ and that $v \equiv 0$ is a solution of this equation. Thus, because of (3.21), $v'(t;w)$ is always negative and $v(\cdot;w)$ is strictly decreasing. Since $v \equiv 0$ is a solution of (3.20), $v(t;w)$ remains positive for $t \geqslant 0$. Therefore, $v(t;w) \in (0,1]$ $\forall t \geqslant 0$; this proves the existence and uniqueness of v and the monotonicity in t.

For the monotonicity in w, fix $w_1 > w_2 \geqslant 0$. Then $v'(0;w_1) = -(\sqrt{w_1} + 1) < v'(0,w_2) = -(\sqrt{w_2} + 1)$, and $v(t;w_1) < v(t;w_2)$ for small $t > 0$. Suppose that there exists a $t^* > 0$ such that $v(t^*;w_1) = v(t^*;w_2)$; then $v'(t^*;w_1) \geqslant v'(t^*;w_2)$, which leads to a contradiction with $w_1 \leqslant w_2$. This completes the proof of part 1 of the Lemma.

Because $v(t;w) > 0$ we have

$$v'(t;w) < -v(t;w)^2\sqrt{A^2t^2 + w},$$

or

$$\left(\frac{1}{v(t;w)}\right)' > \sqrt{A^2t^2 + w}. \tag{4.2}$$

We integrate (4.2) from 0 to t and apply the initial condition $v(0;w) = 1$ to find the following estimate of $v(t;w)$:

$$v(t;w) < \frac{2A}{2A + At\sqrt{A^2t^2 + w} + w\log\left(\frac{At + \sqrt{A^2t^2 + w}}{\sqrt{w}}\right)} < \frac{2}{2 + t\sqrt{A^2t^2 + w}}.$$

This estimate proves part 2 and shows that $v(t;w) \to 0$ as $t \to \infty$.

The right-hand side of (3.20) depends continuously on w. This together with the estimate (4.1) of $v(t;w)$ at $t = \infty$ proves part 3. □

In order to solve (3.20)–(3.23), we need to find w for which (3.22)–(3.23) are satisfied. Knowing a correct value of w, we can obtain a solution $v(t)$ which leads to a solution of the original problem (2.11)–(2.16). Therefore, next we concentrate on finding a correct w.

Definition 2 We define a function $I : [0,\infty) \to [0,\infty)$ in the following way. For given $w \in [0,\infty)$ let $v(\cdot,w)$ be the solution of (3.20)–(3.21) given by Lemma 1. By items 1 and 2 of Lemma 1 there exists a unique $t_{\text{end}}(w) \geqslant 0$ satisfying

$$v(t_{\text{end}}(w);w) = v_{\text{nozzle}}. \tag{4.3}$$

Define $I(w)$ as

$$I(w) = \int_0^{t_{\text{end}}(w)} \frac{Atv(t;w)}{\sqrt{A^2t^2 + w}}\, dt. \tag{4.4}$$

By Lemma 1, part 2 the integrable function is bounded from above and the integral converges.

Corollary 3 *Solving* (3.20)–(3.23) *is equivalent to finding a* $w \geqslant 0$ *that satisfies*

$$I(w) = \text{Re}. \tag{4.5}$$

In the next three lemmas we will show some properties of $I(w)$, which lead to a characterization of existence and uniqueness of a solution to (4.5).

Lemma 4 $I(w)$ *is a strictly decreasing function of* w.

Proof Choose w_1 and w_2 with

$$w_1 > w_2 \geqslant 0. \tag{4.6}$$

From part 1 of Lemma 1, it follows that

$$t_{\text{end}}(w_1) < t_{\text{end}}(w_2). \tag{4.7}$$

Combining (4.7) with the statement 1 of Lemma 1 and (4.6) with the definition of $I(w)$, we have

$$\begin{aligned} I(w_1) = \int_0^{t_{\text{end}}(w_1)} \frac{Atv(t;w_1)}{\sqrt{A^2t^2 + w_1}}\, dt &< \int_0^{t_{\text{end}}(w_2)} \frac{Atv(t;w_1)}{\sqrt{A^2t^2 + w_1}}\, dt \\ &< \int_0^{t_{\text{end}}(w_2)} \frac{Atv(t;w_2)}{\sqrt{A^2t^2 + w_2}}\, dt = I(w_2), \end{aligned}$$

which proves the lemma. □

Lemma 5 $I(w)$ *is continuous.*

Proof Fix $w \geqslant 0$ and let

$$w_n \to w \quad \text{as} \quad n \to \infty. \tag{4.8}$$

Then

$$\begin{aligned} I(w) - I(w_n) &= \int_0^{t_{\text{end}}(w)} \frac{Atv(t;w)}{\sqrt{A^2t^2 + w}}\, dt - \int_0^{t_{\text{end}}(w_n)} \frac{Atv(t;w_n)}{\sqrt{C^2t^2 + w_n}}\, dt \\ &= \int_0^{t_{\text{end}}(w_n)} \left[\frac{Atv(t;w)}{\sqrt{A^2t^2 + w}} - \frac{Atv(t;w_n)}{\sqrt{A^2t^2 + w_n}} \right] dt + \int_{t_{\text{end}}(w_n)}^{t_{\text{end}}(w)} \frac{Atv(t;w)}{\sqrt{A^2t^2 + w}}\, dt. \\ &= J_1 + J_2. \end{aligned}$$

Both J_1 and J_2 converge to zero as $n \to \infty$; for J_1 this follows from the continuity of $v(t;w)$ in w (Lemma 1) and for J_2 from the continuity of $t_{\text{end}}(w)$ in w, which we prove next.

From Lemma 1 we have that $v(\cdot;w) \in C^1([0,\infty))$ and $-\infty < v_t(t;w) < 0$. Therefore, by the Inverse Function Theorem (e.g. [12, Theorem 9.24]) there exists a function $t = t(\cdot;w) \in C^1((0,1])$ such that $t\big(v(\tilde{t};w);w\big) = \tilde{t}$ for all $\tilde{t} \geqslant 0$.

Next note that

$$v_n := v(t_{\text{end}}(w_n);w) \longrightarrow v_{\text{nozzle}} \quad \text{as} \quad n \to \infty, \tag{4.9}$$

since

$$\begin{aligned} |v(t_{\text{end}}(w_n);w) - v_{\text{nozzle}}| &= |v(t_{\text{end}}(w_n);w) - v(t_{\text{end}}(w_n);w_n)| \\ &\leqslant \|v(\cdot;w) - v(\cdot;w_n)\|_\infty \longrightarrow 0 \end{aligned}$$

by part 3 of Lemma 1. Therefore, by continuity of $t(\cdot;w)$ we have

$$t_{\text{end}}(w_n) = t\big(v(t_{\text{end}}(w_n);w);w\big) = t(v_n;w) \longrightarrow t(v_{\text{nozzle}};w) = t_{\text{end}}(w),$$

which completes the proof. □

Lemma 6 $\lim_{w\to\infty} I(w) = 0$.

Proof From the definition of $I(w)$ and $v(t;w) \in (0,1]$ (Lemma 1) we have

$$\begin{aligned} I(w) &= \int_0^{t_{\text{end}}(w)} \frac{Atv(t;w)}{\sqrt{A^2t^2+w}}\,dt < \int_0^{t_{\text{end}}(w)} \frac{At}{\sqrt{A^2t^2+w}}\,dt \\ &= \frac{\sqrt{w + A^2 t_{\text{end}}(w)^2} - \sqrt{w}}{A} = \frac{At_{\text{end}}(w)^2}{\sqrt{w + A^2 t_{\text{end}}(w)^2} + \sqrt{w}}. \end{aligned}$$

Because $t_{\text{end}}(w)$ decreases in w, by letting $w \to \infty$ we find

$$\lim_{w\to\infty} I(w) = 0.$$

□

Summarizing the results of previous lemmas, we formulate a theorem of existence and uniqueness of a solution to the original problem (2.11)–(2.16).

Theorem 7 *There exists a solution to the problem* (2.11)–(2.16) *if and only if*

$$I(0;A,v_{\text{nozzle}}) > \text{Re}. \tag{4.10}$$

If it exists, the solution is unique.

The theorem follows simply from Lemmas 4, 5, and 6.

In Section 5, we describe two algorithms for computing $I(0;A,v_{\text{nozzle}})$ as a function of A and v_{nozzle}, resulting in the graph of Fig. 5. As a consequence of Theorem 7, a solution to the original problem (2.11)–(2.16) exists only if the point $(A, v_{\text{nozzle}}, \text{Re})$ is below the surface $I(0;A,v_{\text{nozzle}})$.

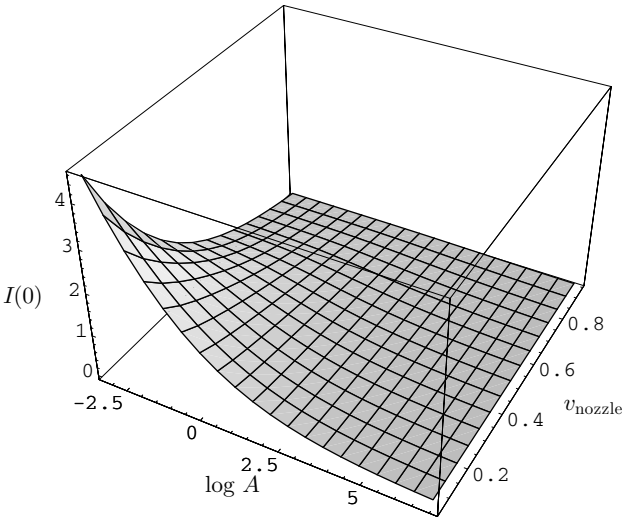

FIGURE 5. Surface $I(0; A, v_{\text{nozzle}})$.

5 Numerical aspects

The problem of this paper gives rise to two slightly different numerical questions. The first question arises in making a phase diagrams (see Fig. 9); in order to distinguish between existence and non-existence of a curved jet we need to calculate $I(0; A, v_{\text{nozzle}})$ and check the existence condition $I(0; A, v_{\text{nozzle}}) > \text{Re}$ (see (4.10)). The second question arises when this condition is fulfilled: by Corollary 3 we then need to find $w > 0$ such that $I(w; A, v_{\text{nozzle}}) = \text{Re}$, from which v and Θ can then be determined by solving (3.20)–(3.21) and using (3.19).

The main differential equation (3.20) can be solved either analytically or numerically, giving rise to two different methods.

Method 1. When $w = 0$, it is possible to solve the problem (3.20)–(3.21) analytically (Appendix A). The rescaled domain size z^* is then to be determined implicitly from

$$v_{\text{nozzle}} = \frac{(2A)^{1/3}}{(3z^*)^{2/3}} \left(1 + \left(\frac{J_{\frac{2}{3}}(z^*)c_1 - J_{-\frac{2}{3}}(z^*)}{J_{\frac{1}{3}}(z^*) + J_{-\frac{1}{3}}(z^*)c_1} \right)^2 \right)^{-1}, \quad c_1 = \frac{J_{-\frac{2}{3}}(\sqrt{2A}/3)}{J_{\frac{2}{3}}(\sqrt{2A}/3)}, \tag{5.1}$$

where the J_α are the Bessel functions of the first kind. We then calculate $t_{\text{end}}(0)$ and $I(0; A, v_{\text{nozzle}})$ as

$$t_{\text{end}}(0) = \frac{(6z^*)^{1/3}}{A^{2/3}} \frac{J_{\frac{2}{3}}(z^*)c_1 - J_{-\frac{2}{3}}(z^*)}{J_{\frac{1}{3}}(z^*) + J_{-\frac{1}{3}}(z^*)c_1}, \tag{5.2}$$

$$I(0; A, v_{\text{nozzle}}) = \frac{1 - v_{\text{nozzle}}}{v_{\text{nozzle}}} - A\frac{t_{\text{end}}(0)^2}{2}. \tag{5.3}$$

This method only is available for the special case $w = 0$ and can only be used for making phase diagrams and checking the existence condition (4.10).

Method 2. Alternatively, one may integrate (3.20) numerically until the condition $v(t;0) = v_{\text{nozzle}}$ is reached. The integral $I(w; A, v_{\text{nozzle}})$ can be computed numerically as well. This method is available for all $w \geqslant 0$.

We solve (4.5) by the bisection method, supplemented with an upper bound on w that follows from the estimate (4.1): since for all w,

$$v(t;w) < \frac{2}{At^2},$$

we have

$$v_{\text{nozzle}} = v(t_{\text{end}}(w);w) < \frac{2}{At_{\text{end}}(w)^2},$$

and therefore $At_{\text{end}}(w)^2 < 2/v_{\text{nozzle}}$. We thus estimate

$$I(w; A, v_{\text{nozzle}}) = \int_0^{t_{\text{end}}(w)} \frac{Atv(t;w)}{\sqrt{A^2t^2 + w}}\, dt < \frac{At_{\text{end}}(w)^2}{2\sqrt{w}} < \frac{1}{v_{\text{nozzle}}\sqrt{w}}. \tag{5.4}$$

Therefore, the solution w of (4.5) satisfies the *a priori* estimate

$$w \leqslant \frac{1}{v_{\text{nozzle}}^2 \text{Re}^2},$$

which together with the existence condition (4.10) gives the initial interval for the bisection method

$$w \in \left[0, 1/(v_{\text{nozzle}}\text{Re})^2\right].$$

6 Results

From Theorem 7, it follows that if the parameters A, Re, and v_{nozzle} satisfy (4.10), then there exists a solution to the stationary curved jet equations (2.5)–(2.10) (or equivalently (3.20)–(3.23)). For a numerical experiment, we take parameter values such that (4.10) is satisfied. By changing one of the model parameters such that the point (A, Re, v_{nozzle}) approaches the boundary of the existing region, we investigate the change in the shape of the jet.

As a reference configuration for the numerical experiments shown below we consider syrup with viscosity $\eta = 3.2\,\text{Pa s}$ and density $\rho = 1000\,\text{kg/m}^3$ (typical of pancake syrup) pouring from the height $L = 2 \times 10^{-2}\,\text{m}$. The velocities of the belt and the flow at the nozzle are $v_{\text{belt}} = 0.5\,\text{m/s}$ and $v_{\text{nozzle}} = 0.05\,\text{m/s}$, respectively. Figure 6 shows curves in non-dimensional parameter space $(A, v_{\text{nozzle}}, \text{Re})$ corresponding to variation of a single (dimensional) physical parameter L, ν, v_{belt}, or v_{nozzle}. In the figure, we see that upon decreasing ν or v_{belt}, or increasing L or v_{nozzle}, the point $(A, v_{\text{nozzle}}, \text{Re})$ eventually leaves the region $\{(A, v_{\text{nozzle}}, \text{Re}) : I(0; A, v_{\text{nozzle}}) > \text{Re}\}$. The numerically calculated shapes become vertical as the parameters approach the boundary. In Fig. 7, we present the shapes of the jet for specific values of the parameters along each of these curves.

For a point $(A, v_{\text{nozzle}}, \text{Re})$ at the boundary of the existence region, the solution w of (4.5) equals 0. Then a jet solution exists provided we drop the tangency condition (2.9); the jet is then exactly vertical ($\Theta = \pi/2$) (see (3.19)). Note that both the curved and the purely vertical ($w = 0$) jets are under tension (part 1 of Lemma 1).

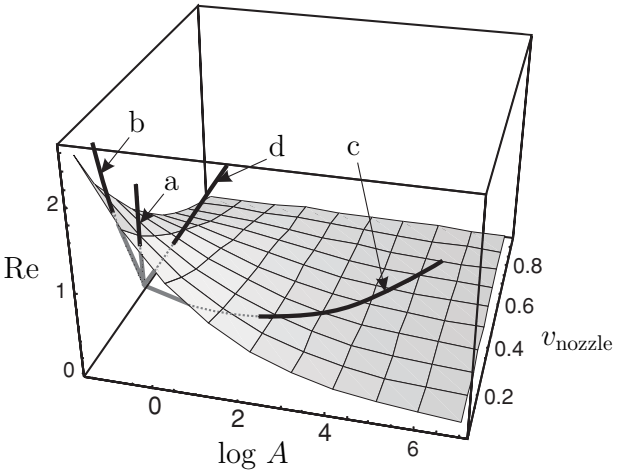

FIGURE 6. Curves in non-dimensional parameter space $(A, v_{\text{nozzle}}, \text{Re})$ as we change one of the process parameters $(L, \nu, v_{\text{belt}}, v_{\text{nozzle}})$. The grey parts of the curves below the surface $I(0; A, v_{\text{nozzle}})$ correspond to the curved jet; we conjecture that the black parts of the traces correspond to a vertical jet. Line a: increasing L; line b: decreasing ν; line c: decreasing v_{belt}; and line d: increasing v_{nozzle}.

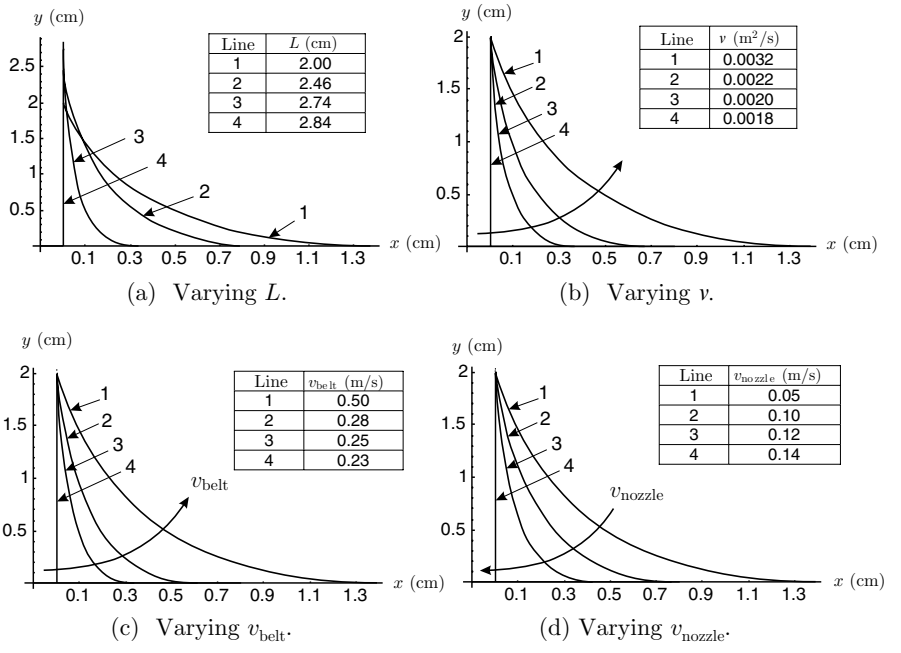

(a) Varying L. (b) Varying ν.

(c) Varying v_{belt}. (d) Varying v_{nozzle}.

FIGURE 7. The shapes of a jet for different values of the process parameters $(L, \nu, v_{\text{belt}}, v_{\text{nozzle}})$. The reference values for the parameters are $\eta = 3.2\,\text{Pa s}$, $\rho = 1000\,\text{kg/m}^3$, $L = 2 \times 10^{-2}\,\text{m}$, $v_{\text{belt}} = 0.5\,\text{m/s}$, and $v_{\text{nozzle}} = 0.05\,\text{m/s}$.

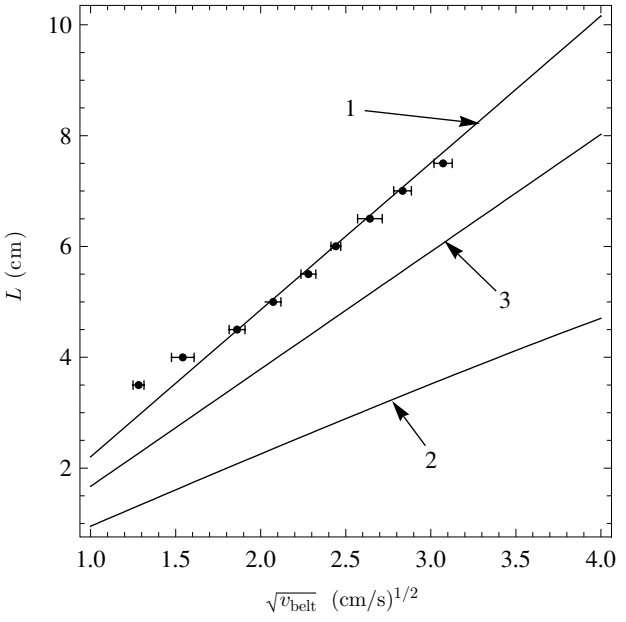

FIGURE 8. The experimental results of [2], experiment 7 (dots) for the steady–unsteady boundary, and a linear fit (line 1); the border of the curved-jet existence region predicted by our model (line 2); and the steady–unsteady boundary predicted by the model of [2] (line 3). The jet is stable under line 1, and predicted to be curved under line 2 and stable under line 3.

Summarizing the numerical experiments, we observe that by increasing the flow velocity at the nozzle or the distance between the belt and the nozzle the jet shape becomes more vertical; the same is true if we decrease the velocity of the belt or the kinematic viscosity. The jet becomes more vertical when the parameter point $(A, v_{\text{nozzle}}, \text{Re})$ approaches the critical surface $\{I(0; A, v_{\text{nozzle}}) = \text{Re}\}$ and purely vertical if $I(0; A, v_{\text{nozzle}}) = \text{Re}$.

7 Modelling issues

In this section we compare our results with [2, 11] and discuss what happens beyond the curved-jet region.

The general solution behaviour described in the previous section is visible in both the experimental and the theoretical results of [2, 11] (see e.g. [2, Fig. 10] or [11, Fig. 3]).

However, the experimental results of [2] (for instance experiments 5 and 7, shown in [2], Fig. 12) do not distinguish between curved and straight flow, but between steady and unsteady flow. When decreasing the belt velocity, the curved flow first becomes straight, and only later becomes unsteady; therefore the curved–straight transition, as determined by our results, is necessarily a one-sided bound for the steady-unsteady transition. This is illustrated in Fig 8, where the prediction of this paper (line 2) indeed lies below the experimental results of [2, Fig. 12].

Figure 8 also shows a theoretical prediction of the experimental results, derived in [2] by asymptotic means (line 3). Examination of the method, however, shows that this

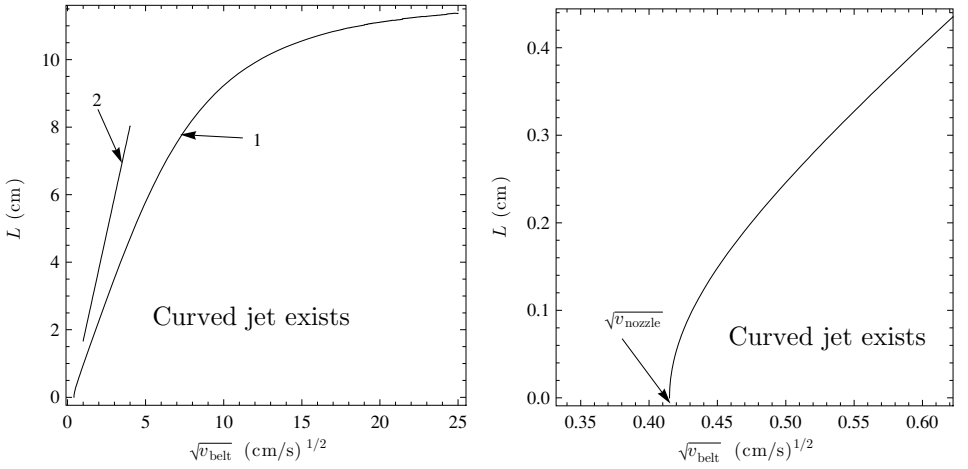

FIGURE 9. The left-hand side figure presents the existence region for the curved-jet solution for different L and $v_{\rm belt}$, predicted by our model (line 1). Line 2 shows the steady–unsteady jet boundary predicted by the model of [2]. The figure on the right-hand side shows a zoom of the existence boundary for the curved-jet solution.

prediction, like the one in this paper, concerns the existence–nonexistence transition of the curved flow solution, and is *a priori* unrelated to the steady–unsteady transition. (In our forthcoming paper [6], we show that the two transitions are necessarily separated from each other in parameter space). Although both line 2 and line 3 are estimates of the same existence–nonexistence transition, they differ because surface tension has been neglected in the present paper.

The asymptotic result of [2] mentioned above also predicts a linear relation between $\sqrt{v_{\rm belt}}$ and L for the existence–nonexistence transition. Figure 9 shows the region of the curved jet obtained for the parameters ν and $v_{\rm nozzle}$ as used in [2], experiment 7 but for a larger range of $v_{\rm belt}$ and L. The linear relation between $\sqrt{v_{\rm belt}}$ and L is reasonable for the values considered in [2], but fails for larger $v_{\rm belt}$ (the curve flattens off), and for $v_{\rm belt}$ close to $v_{\rm nozzle}$ (the curve becomes vertical at $v_{\rm belt} = v_{\rm nozzle}$).

When the model parameters are changed in such a way that the solution w of (4.5) goes to zero then the calculated jet shape becomes close to vertical everywhere, except a small neighbourhood at the contact with the belt. There the jet rapidly bends from almost vertical to horizontal. To capture the jet shape in this bending region the shearing forces and the moment of momentum equation should be included in the model, as shear and bending are significant near the boundary [11]. However, including these effects in the model will increase the complexity and abandons the possibility of an analytical analysis.

It is an interesting question what happens beyond the existence region for the curved-jet solution in the current model. In the forthcoming paper [6], we investigate the characteristics of the associated dynamic equation, and relate these to the balance between the convective momentum transfer and the momentum transfer due to the longitudinal force in a jet. We show that the vanishing of ξ at the boundary is consistent with the loss of the tangency condition at the belt, implying that the transition to purely vertical flow

is in fact a natural one. However, when the flow from the nozzle increases, the nozzle orientation becomes important, and the jet shape becomes similar to a ballistic trajectory.

The equations for the viscous jet described in this paper are analogous to the equations describing a viscous sheet. Therefore, all the analysis of this paper is true for the fall of viscous sheets onto a moving surface occurring in the modelling of curtain coating [5].

8 Conclusions

In this paper we study a mathematical model of the fall of a viscous jet onto a moving surface. We assume that the jet is falling under gravity and has a curved shape. The model consists of two differential equations, one for the flow velocity and the other for the angle describing the jet's shape. An additional relation fixes the unknown length of the jet.

The initial system of equations is partially solved and then transformed to a first-order differential equation for the velocity. By introducing an additional scalar parameter w the problem is reformulated as an algebraic equation for w (4.5). For this equation, we formulate an existence condition (4.10) and prove uniqueness, thus giving a complete characterization of existence and uniqueness for the original equations. Finally, we solve the equation for w numerically and recover the solution of the original problem.

We have shown that if the existence condition (4.10) is satisfied, then the shape of the jet is convex. Furthermore, the model shows that the curved jet becomes more vertical when: (i) the distance between the nozzle and the surface increases, (ii) the flow velocity at the nozzle increases, (iii) the surface velocity decreases, or (iv) the kinematic viscosity of the fluid decreases. These results correspond with those observed in the basic experiment described in the introduction and in [2].

Appendix A: Calculation of $I(0; A, v_{\text{nozzle}})$

First we calculate $v(t;0)$ analytically. The differential equation for $v(t;0)$ follows from (3.20) and (3.21),

$$v'(t;0) = -v^2(t;0)(At + v(t;0)), \quad v(0;0) = 1. \tag{A 1}$$

By replacing $v(t;0)$ by $Z(t) = 1/v(t;0)$, we find

$$Z'(t)Z(t) = AZ(t)t + 1, \quad Z(0) = 1. \tag{A 2}$$

We seek for a solution of (A 2) in parametric form. With the substitution

$$Z(z) = z + A/2t^2(z), \tag{A 3}$$

where z is a parameter, (A 2) becomes

$$t'(z) = At^2(z) + z, \quad t(1) = 0. \tag{A 4}$$

Here the initial condition is deduced from (A 3) by setting $t(z) = 0$ and $Z(z) = 1$. This differential equation is known as the special Riccati equation [7, p. 4], type 4 and has the

solution

$$t(z) = \frac{\sqrt{2z}\left(J_{\frac{2}{3}}\left(\frac{\sqrt{2A}z^{3/2}}{3}\right)c_1 - J_{-\frac{2}{3}}\left(\frac{\sqrt{2A}z^{3/2}}{3}\right)\right)}{\sqrt{A}\left(J_{\frac{1}{3}}\left(\frac{\sqrt{2A}z^{3/2}}{3}\right) + J_{-\frac{1}{3}}\left(\frac{\sqrt{2A}z^{3/2}}{3}\right)c_1\right)}, \tag{A 5}$$

with

$$c_1 = \frac{J_{-\frac{2}{3}}(\alpha)}{J_{\frac{2}{3}}(\alpha)}, \quad \alpha = \sqrt{2A}/3. \tag{A 6}$$

Here the functions J_α are the Bessel functions of the first kind. The velocity v is given by

$$v(z) = \frac{1}{z}\left(1 + \left(\frac{J_{\frac{2}{3}}\left(\frac{\sqrt{2A}z^{3/2}}{3}\right)c_1 - J_{-\frac{2}{3}}\left(\frac{\sqrt{2A}z^{3/2}}{3}\right)}{J_{\frac{1}{3}}\left(\frac{\sqrt{2A}z^{3/2}}{3}\right) + J_{-\frac{1}{3}}\left(\frac{\sqrt{2A}z^{3/2}}{3}\right)c_1}\right)^2\right)^{-1}. \tag{A 7}$$

To write the result in a more elegant form we replace the parameter z by $\tilde{z} = \sqrt{2A}z^{3/2}/3$ (we then omit tildes)

$$t(z) = \frac{(6z)^{1/3}}{A^{2/3}}\frac{J_{\frac{2}{3}}(z)c_1 - J_{-\frac{2}{3}}(z)}{J_{\frac{1}{3}}(z) + J_{-\frac{1}{3}}(z)c_1}, \tag{A 8}$$

$$v(z) = \frac{(2A)^{1/3}}{(3z)^{2/3}}\left(1 + \left(\frac{J_{\frac{2}{3}}(z)c_1 - J_{-\frac{2}{3}}(z)}{J_{\frac{1}{3}}(z) + J_{-\frac{1}{3}}(z)c_1}\right)^2\right)^{-1}. \tag{A 9}$$

To calculate $t_{\mathrm{end}}(0)$ from the solution (A 8) and (A 9) it is necessary to find z^* satisfying

$$v_{\mathrm{nozzle}} = \frac{(2A)^{1/3}}{(3z^*)^{2/3}}\left(1 + \left(\frac{J_{\frac{2}{3}}(z^*)c_1 - J_{-\frac{2}{3}}(z^*)}{J_{\frac{1}{3}}(z^*) + J_{-\frac{1}{3}}(z^*)c_1}\right)^2\right)^{-1}, \tag{A 10}$$

and then substitute $z = z^*$ into (A 8).

Equation (A 10) has many solutions. A correct solution z^* is the first solution of (A 10) after the point α. It is convenient to search for z^* in the interval (α, z_0) using the bisection method [8]. Here, z_0 is the first zero of $v(z)$ according to (A 9) after the point α.

Next, we have to find a correct z_0. Because zeros of $v(z)$ coincide with zeros of

$$J_{\frac{1}{3}}(z) + J_{-\frac{1}{3}}(z)c_1, \tag{A 11}$$

we can look for the first zero of (A 11) after α. Using (A 6), we can rewrite the latter as

$$J_{\frac{1}{3}}(z_0)J_{\frac{2}{3}}(\alpha) + J_{-\frac{1}{3}}(z_0)J_{-\frac{2}{3}}(\alpha) = 0. \tag{A 12}$$

This equation can be rewritten in terms of Airy functions 1, 10.4.22 and 10.4.27 as

$$Bi(-\hat{z}_0)Ai'(-\hat{\alpha}) - Ai(-\hat{z}_0)Bi'(-\hat{\alpha}) = 0, \ \hat{z}_0 = \left(\frac{3z_0}{2}\right)^{\frac{2}{3}}, \ \hat{\alpha} = \left(\frac{3\alpha}{2}\right)^{\frac{2}{3}}. \tag{A 13}$$

Using the representation of Airy functions via modulus and phase [1, 10.4.69 and 10.4.70]

$$Ai(-\hat{z}_0) = M(\hat{z}_0)\cos\theta(\hat{z}_0), \quad Bi(-\hat{z}_0) = M(\hat{z}_0)\sin\theta(\hat{z}_0),$$
$$Ai'(-\hat{\alpha}) = N(\hat{\alpha})\cos\phi(\hat{\alpha}), \quad Bi'(-\hat{\alpha}) = N(\hat{\alpha})\sin\phi(\hat{\alpha}),$$

we see that (A 13) becomes

$$\sin(\theta(\hat{z}_0) - \phi(\hat{\alpha})) = 0. \tag{A 14}$$

For large $\hat{z}_0 \gg 1$ and $\hat{\alpha} \gg 1$, the asymptotic expressions for $\theta(\hat{z}_0)$ and $\phi(\hat{\alpha})$ [1, 10.4.79 and 10.4.81] are given by

$$\theta(\hat{z}_0) = \frac{\pi}{4} - \frac{3}{2}\hat{z}_0^{2/3}\left(1 - \frac{5}{32\hat{z}_0^3} + \frac{1105}{6144\hat{z}_0^6} + \cdots\right),$$

and

$$\phi(\hat{\alpha}) = \frac{3\pi}{4} - \frac{3}{2}\hat{\alpha}^{2/3}\left(1 + \frac{7}{32\hat{\alpha}^3} - \frac{1463}{6144\hat{\alpha}^6} + \cdots\right),$$

or in terms of z_0 and α (A 13)

$$\theta(z_0) = \frac{\pi}{4} - z_0\left(1 - \frac{5}{72z_0^2} + \frac{1105}{31104z_0^4} + \cdots\right), \tag{A 15}$$

and

$$\phi(\alpha) = \frac{3\pi}{4} - \alpha\left(1 + \frac{7}{72\alpha^2} - \frac{1463}{31104\alpha^4}\right). \tag{A 16}$$

After substituting (A 15) and (A 15) into (A 14) for $\alpha \gg 1$ we find

$$z_0 \approx \alpha + \pi/2. \tag{A 17}$$

When α is not large we can find z_0 numerically by looking for a solution of (A 12) in the interval $(\alpha, \alpha + \pi)$.

Once z_0 is found we find z^* and consequently compute $t_{\text{end}}(0)$. Knowing $t_{\text{end}}(0)$, we can compute $I(0)$. To avoid computation of the integral

$$I(0) = \int_0^{t_{\text{end}}(0)} v(t;0)\,dt,$$

we can calculate this integral using the differential equation (A 1), when written as

$$\left(\frac{1}{v(t;0)}\right)' = At + v(t;0). \tag{A 18}$$

By integrating this equation from 0 to $t_{\text{end}}(0)$, we get

$$\left(\frac{1}{v(t_{\text{end}}(0);0)} - \frac{1}{v(0;0)}\right) = A\frac{t_{\text{end}}(0)^2}{2} + \int_0^{t_{\text{end}}(0)} v(t;0)\,dt. \tag{A 19}$$

We use the definitions of $I(0)$ and $t_{\text{end}}(0)$, together with the initial condition $v(0;0) = 1$ to

obtain

$$I(0) = \frac{1 - v_{\text{nozzle}}}{v_{\text{nozzle}}} - A\frac{t_{\text{end}}(0)^2}{2}. \tag{A 20}$$

References

[1] Abramowitz, M. & Stegun, I. A. (1964) *Handbook of Mathematical Functions with Formulas, Graphs, and Mathematical Tables*, volume 55 of *National Bureau of Standards Applied Mathematics Series*. For sale by the Superintendent of Documents, U.S. Government Printing Office, Washington, D.C.

[2] Chiu-Webster, S. & Lister, J. R. (2006) The fall of a viscous thread onto a moving surface: a 'fluid-mechanical sewing machine'. *J. Fluid Mech.*, **569**, 89–111.

[3] Coddington, E. A. & Levinson, N. (1955) *Theory of Ordinary Differential Equations*. McGraw-Hill, New York-Toronto-London.

[4] Cruickshank, J. O. (1980) *Viscous Fluid Buckling: A Theoretical and Experimental Analysis with Extensions to General Fluid Stability*. PhD thesis, Iowa State University, Ames IA, USA.

[5] Dyson, R. J. Howell, P. D. Breward, C. J. W. Herdman, P. & Brander, J. (2005) Mathematical modelling of curtain coating. In: *Proceedings of the 6th European Coating Symposium ECS2005*.

[6] Hlod, A., Aarts, A. C. T., van de Ven, A. A. F. & Peletier, M. A. Boundary conditions for the three flow regimes of a viscous jet falling onto a moving surface, in preparation.

[7] Polyanin, A. D., Zaitsev, V. F. & Moussiaux, A. (2002) *Handbook of First Order Partial Differential Equations*, volume 1 of *Differential and Integral Equations and Their Applications*. Taylor & Francis, London.

[8] Quarteroni, A., Sacco, R. & Saleri, F. (2000) *Numerical Mathematics*, volume 37 of *Texts in Applied Mathematics*. Springer-Verlag, New York.

[9] Ribe, N. M. (2003) Periodic folding of viscous sheets. *Phys. Rev. E*, **68**, 036305.

[10] Ribe, N. M. (2004) Coiling of viscous jets. *Proc. R. Soc. London A*, **460**, 3223–3239.

[11] Ribe, N. M., Lister, J. R. & Chiu-Webster, S. (2006) Stability of a dragged viscous thread: Onset of stitching in a fluid-mechanical sewing machine. *Phys. Fluids*, **18**, 124105 (2006) (8 pages).

[12] Rudin, W. (1976) *Principles of Mathematical Analysis*. McGraw-Hill, New York, 3rd ed., International Series in Pure and Applied Mathematics.

[13] Skorobogatiy, M. & Mahadevan, L. (2000) Folding of viscous sheets and filaments. *Europhys. Lett.*, **52**(5), 532–538.

[14] Taylor, G. I. (1969) Instability of jets, threads, and sheets of viscous fluid. In *Proceedings of the 12th International Congress of Applied mechnaics (Stanford, 1968)*, pp. 382–388. Springer-Verlag, New York.

[15] Tchavdarov, B. M., Yarin, A. L. & Radev, S. (1993) Buckling of thin liquid jets. *J. Fluid Mech.*, **253**, 593–615.

[16] Yarin, A. L. (1993) *Free Liquid Jets and Films: Hydrodynamics and Rheology*. Interaction of Mechanics and Mathematics Series. Longman Scientific & Technical, Harlow.

[17] Yarin, A. L. & Tchavdarovz, B. M. (1996) Onset of folding in plane liquid films. *J. Fluid Mech.*, **307**, 85–99.